European Journal of Pharmaceutics and Biopharmaceutics 73 (2009) 331–336

Contents lists available at ScienceDirect

European Journal of Pharmaceutics and Biopharmaceutics

journal homepage: www.elsevier.com/locate/ejpb

Research paper

Sculptured drug-eluting stent for the on-site delivery of tacrolimus

Paola Minghetti [a,*], Francesco Cilurzo [a], Francesca Selmin [a], Antonella Casiraghi [a], Andrea Grignani [b], Luisa Montanari [a]

[a] Dipartimento di Scienze Farmaceutiche "P. Pratesi", Università degli Studi di Milano, Milan, Italy
[b] CID S.r.L., Strada per Crescentino, Saluggia, Italy

ARTICLE INFO

Article history:
Received 9 April 2009
Accepted in revised form 12 August 2009
Available online 15 August 2009

Keywords:
Drug-eluting stent
Janus *Carbo*Stent
Tacrolimus
AFM

ABSTRACT

This work aimed to evaluate the flexibility of a novel pyrolytic carbon coated drug-eluting stent platform, which presents the peculiarity of deep sculptures realized on the stent's outer surface (reservoirs). Tacrolimus (TCR) or TCR/excipient mixtures were loaded into the reservoirs, and their permanence into stent's reservoirs was verified by an in vitro short-time release test in human blood. Moreover, the impact of the excipients on the TCR physical state and surface morphology of the reservoirs and the release kinetics were studied. The reservoirs resulted homogeneously filled. Upon exposure to blood, no loss of materials from reservoirs was observed, and the drug release after 15 min was negligible in all cases. The loading procedure caused the drug amorphization and, AFM revealed that the surfaces were smooth and homogeneous with the exception of the TCR/poloxamer 188 mixture where spatial oriented crystals were evident. Poly(N-vinyl pyrrolidone) improved the in vitro TCR release rate constants (*K*). Poly(methylmethacrylate) (PMM) significantly reduced the *K* value both in vitro and in vivo. Indeed, the in vivo drug concentrations in rabbit artery wall significantly decreased, decreasing the TCR/PMM ratio. The characteristics of the stent strut resulted suitable to load material with different physicochemical characteristics.

1. Introduction

Coronary stent implantations have revolutionized the practice of interventional cardiology [1] becoming the standard care for the treatment of coronary lesions. However, in-stent restenosis [2,3] as well as thrombosis [4] remains the main adverse cardiac events associated to high rates of morbidity and mortality. In order to reduce in-stent restenosis, drug-eluting stents (DESs) have been emerged as an appealing solution to localize drug delivery [5]. In particular, the on-site drug administration obtained by DES has shown significant benefits in suppressing neointimal proliferation and/or preventing inflammation by a sustained release of anti-proliferative and/or anti-inflammatory drugs at injured arterial tissue minimizing the systemic adverse effects [6,7]. Among the available technologies, two main approaches can be individuated to load a drug on the stent surface.

The former is based on the incorporation of a drug in the polymeric film used to coat the stent surface; in the latter, the drug is directly deposited onto the stent surface avoiding the aid of excipients [8]. This approach was followed in the development of Janus *Carbo*Stent™ [9], which presents the peculiarity of deep sculptures (Fig. 1) realized on the stent's external surface loaded by tacrolimus (TCR), a 23-member macrolide lactone with potent immunosuppressive activity. Even if the efficacy of Janus *Carbo*Stent™ has been proven and discussed [9–11], few information about the technological characteristics of this type of DES are available in literature. Indeed, besides the loading of paclitaxel onto the stent struts [12], the use of different drugs as the only component or their mixtures with an excipient has not been evaluated for assessing the feasibility of this platform.

The adhesion of a material to stent surface is a critical issue as far as the safety and the efficacy is concerned. As an example, one drawback of embedding the drug in the polymeric coat is the risk that the coating may spall from the stent substrate due to high mechanical strains that the stent suffers during its deployment [13,14].

The present work aimed to evaluate the flexibility of the *Carbo*Stent™ platform by studying the effects of blending TCR with several excipients on the main critical issues in the DES development, namely drug release kinetic and permanence of the loaded material into the stent's reservoirs. TCR or TCR/excipient mixtures were loaded into the reservoirs, and their permanence was verified by an in vitro short-time release test in human blood. Indeed, the permanence of filling into the stent's reservoirs would be perturbed only by low hemodynamic stress, as the sculptures of the

* Corresponding author. Dipartimento di Scienze Farmaceutiche "P. Pratesi", Università degli Studi di Milano, via G. Colombo, 71-20133 Milan, Italy. Tel.: +39 (0)2 503 24639; fax: +39 (0)2 503 24657.
E-mail address: paola.minghetti@unimi.it (P. Minghetti).

0939-6411/$ - see front matter © 2009 Elsevier B.V. All rights reserved.
doi:10.1016/j.ejpb.2009.08.004

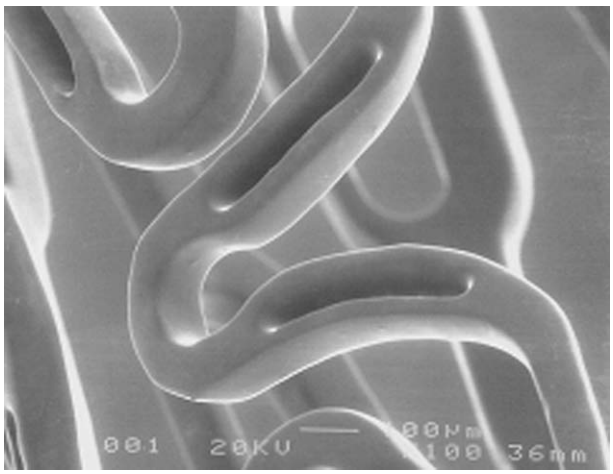

Fig. 1. Microphotography of sculptured drug-eluted stent.

stent were designed in order to be not affected by the radial forces and flexibility during the stent expansion and upon its deployment. Poly(methyl methacrylate), poly(N-vinyl pyrrolidone) or poloxamer 188 were tested in order to prolong or increase the TCR release rate both in vitro and in vivo. Finally, the effects of the selected materials on the TCR solid state and surface roughness of the filled reservoirs were also considered worthy of investigation. An in-deep understanding of the TCR solid state is desirable not only to fully characterize this type of DES, but also to provide information on the drug physicochemical properties, which are scantly investigated [15–17].

2. Materials and methods

2.1. Materials

Tacrolimus (TCR, Astellas Pharma Inc., Osaka, J); poly(methyl methacrylate) (PMM, VISTA-OPTICS, UK); poloxamer 188, (p188, Lutrol® 188, BASF, UK); poly(N-vinyl pyrrolidone) PVP 17PF (PVP) (BASF, UK). All solvents were of analytic grade, unless specified.

2.2. Stent design

The peculiarity of the *Carbo*Stent™ platform consists in the presence of sculptures on stent's outer surface that can be loaded with a drug. The stent strut is dig on the outer surface to create unique sculptures (Fig. 1). Drug sculpture locations are selected according to a homogeneous mapping designed through the use of the finite element analysis to guarantee a uniform distribution of the drug into the vessel tissue and optimize the mechanical properties of the stent platform (data not shown). Their existence on the stent struts does not affect stent radial force and flexibility. The overall stent surface, including sculptures, is coated with a high-density ultrathin film of pyrolytic carbon (*Carbo*film™). The technique used for the coating is a physical vapor deposition process where groups of carbon atoms are transferred from a pyrolytic turbostatic carbon target to the substrate to be coated. This process is carried out in high-vacuum conditions, which prevent from any chemical reaction. Pyrolytic carbon was selected as it assures high strength and resistance to fatigue with thromboresistance and blood compatibility [9]. The composition of TCR or the TCR/excipient mixtures is reported in Table 1, and the nominal loading was set to 230 μg. To load a formulation onto DES, the micronized compounds were mechanically inserted into the reservoirs, after having thoroughly mixed. Then, the mixtures were settled to their final homogenous form by means of solvent dispensing. The suitability of the loading procedure was verified by observing the sculptures and surface of the stent strut by optical microscopy (10×, Axiscope, Zeiss, G). Misplacements or excesses of the mixture were mechanically removed from the surface of the stent.

2.3. TCR physical state characterization

2.3.1. Powder X-ray diffraction

The physical state of TCR and the corresponding mixtures were evaluated on the materials deposed on a flat pyrolytic carbon surface (*Carbo*film™) following the same procedure used in stent loading. Powder X-ray diffraction spectra of TCR and TCR/excipient mixtures were collected by using a Rigaku DMAX powder diffractometer (Rigaku, J) with Cu K radiation and a monochromator on the diffracted beam.

2.3.2. ATR–FTIR spectroscopy

TCR and the TCR/excipient mixtures deposed on a flat pyrolytic carbon surface (*Carbo*film™) were placed on a diamond crystal mounted on the ATR cell (Perkin Elmer, Monza, I) of a FTIR (SpectrumTM One, Perkin Elmer, Monza, I). The spectra were recorded at 2 cm^{-1} resolution, and 16 scans were collected over the wave number region 4000–650 cm^{-1}.

2.3.3. Differential scanning calorimetry

DSC data of samples were recorded by using a DSC Q100 TA Instruments (TA Instruments, New Castle, USA). The samples were sealed in aluminum pans and heated in inert atmosphere (50 mL/min N_2). The reference was an empty pan. The equipment was calibrated with an indium sample. The samples were cycled at 5 K/min from 20 °C to 160 °C, cooled at 5 K/min to −20 °C and reheated at 5 K/min to 160 °C under nitrogen purging (50 mL/min). First cycle has been run to erase the thermal history and eliminate the residual water, the second heating cycle has always been considered to determine the glass transition temperature (T_g). All determinations were performed in duplicate.

2.3.4. Atomic force microscopy

The morphologies of TCR and the TCR/excipient mixtures loaded into the DES were observed using atomic force microscopy (AFM) analysis. AFM images were recorded with a Multimode-

Table 1
Composition (%, w/w) of the drug/excipient mixtures loaded onto sculptures and in vitro TCR release rate constants (K) calculated according to the Higuchi's equation.

Components	Composition (%, w/w)					
	1	2	3	4	5	6
TCR	100	67	33	67	80	67
PMM	–	33	67	–	–	–
p188	–	–	–	33	–	–
PVP	–	–	–	–	20	33
K ($h^{-0.5}$ ± SD)	0.241 ± 0.023	0.074 ± 0.005	0.037 ± 0.008	0.332 ± 0.100	0.211 ± 0.040	0.591 ± 0.028

Nanoscope IV AFM microscope (Veeco Instruments, USA) operated in the tapping mode in air. Typical environmental conditions were: relative humidity: 35–40% and temperature: 22–24 °C. The qualitative physicochemical characterization was carried out performing phase imaging simultaneously to standard topographical imaging. The phase imaging technique typically provides a contrast based on non-homogeneous chemical–physical–mechanical properties on the surface.

2.4. In vitro TCR release

2.4.1. In vitro TCR release testing

In vitro release testing was carried out in screwed-glass vials shaken in a water-bath shaker at 100 rpm and 37.0 ± 0.1 °C. The stents were immersed in 4 mL pH 7.4 PBS containing 0.05% w/v sodium dodecyl sulfate (SDS). The addition of a surfactant to the buffer was compulsory in order to increase the aqueous solubility of TCR and maintain the sink condition throughout the testing. At pre-determined intervals, the entire dissolution medium was withdrawn to assure sink condition during dissolution testing. The amount of the TCR released was determined by the HPLC–UV method reported in Section 2.5.1. At the end of in vitro release testing, the complete recovery of TCR was assessed by a mass balance evaluation. In addition, the sculptures and surface of the stent strut were visually observed by optical microscopy (10×, Axiscope, Zeiss, G). The results are expressed as mean ± standard deviation of three determinations.

2.4.2. Loss of TCR in human blood

The loss of TCR in full human blood was measured after 5, 10 and 15 min of incubation. These data points were selected on the basis of the estimated period of contact between the collapsed stent and the blood during the DES delivering in the artery wall using a guiding catheter before the ballooning and the deployment procedure. The stents were incubated in 4 mL heparinized human blood in screwed vials and shaken at the frequency of 100 rpm and 37 ± 0.1 °C. At the pre-determined intervals, DESs were withdrawn, gently soaked and washed in 2 mL HPLC water. Then, the stents were placed in flasks containing 5 mL acetonitrile after observation by optical microscopy to verify the absence of blood residues that can coagulate and form a thin film, which affects the solubilization of the residual drug. Immediately before HPLC analysis, an aliquot of 0.5 mL was withdrawn and diluted with the same volume of HPLC water. TCR concentration was determined by the HPLC–UV method described in Section 2.5.1.

2.4.3. In vivo TCR determination after DES deployment

All animal experiments complied with the Italian law (D.L. n. 116 of 27 January 1992) and associated guidelines in the European Communities Council Directive of 24 November 1986 (86/609 ECC). New Zealand white rabbits ($n = 3$) were randomly assigned to receive one DES per iliac artery at nominal pressure with 30 s of balloon inflation. The expanded stents had a diameter of 3 mm. The experiments were conducted by using the DES loaded with TCR or TCR/PMM mixture. At day 3 after having received 1000 units of heparin, the animals were euthanized; the blood and the stented vessels were collected. The stented segment of the artery was excised along with a 5 mm-long arterial segment proximal and distal to the stent. The stent was carefully removed from the arterial tissue. Tissue samples were homogenized, centrifuged and separated by solid phase extraction (Bond Elut C18–Varian cartridges). The TCR content (recovery) in the stent and arterial tissue were determined by the HPLC/MS/MS method as described in Section 2.5.2.

2.5. HPLC analyses

2.5.1. HPLC–UV method

The following HPLC assay was developed: an Agilent 1100 HPLC system was used to determine drug concentration (1100 autosampler, 1100 quaternary pump with degasser, 1100 thermostated column compartment, and 1100 diode array detector) (Agilent, Palo Alto, CA).

A Waters Spherisorb® ODS2 C-18 was used as the stationary phase (150 × 4.6 mm, Vimodrone, I), and a combination of water with acetonitrile and phosphoric acid (40/60/1%, v/v) was used as the mobile phase. The flow rate was controlled at 2.0 mL/min. The effluent was monitored at 215 nm for 8 min. Total run time was 7 min and the retention times for the pure TCR and the tautomer #1 were 5.6 min and 4.4 min, respectively. To optimize the quantification and the resolution of TCR peaks, two different volumes were injected:

20 μL: standard calibration curves ranged from 0.5 to 10 g/mL ($r^2 = 0.99927$);
60 μL: standard calibration curves ranged from 5 to 10 g/mL ($r^2 = 0.99983$).

2.5.2. HPLC MS/MS method

TCR in tissue samples was analyzed by a HPLC MS/MS method. Experimental conditions: column 2.0 × 150 mm Phenomenex 5 μm Prodigy ODS3; MS detector (Applied Biosystems API 3000) with ESI Ion source Turbolon Spray; mobile phase: 0.1 mM ammonium acetate in methanol; flow rate 0.2 mL/min; injection volume: 10 μL; ion detected m/z: 821.6 and 768.0. The standard calibration curve ranged from 5 to 2500 pg/mg of tissue ($r^2 = 0.9922$).

3. Results and discussion

3.1. Adhesion of the TCR mixtures onto the stent

The observation of the DESs by optical microscopy revealed that all reservoirs were homogeneously loaded with the drug/excipient mixtures and appeared as a glass. Moreover, no traces of the drug or the mixtures were found on the outer surface of the stent struts indicating that the current procedure is suitable to load blends with different physicochemical characteristics. As an example, Fig. 2a and c shows how Stent 1 and Stent 2 appear at the end of the loading procedure, respectively.

Upon exposure to blood in the selected hydrodynamic condition (100 rpm), the sculptures did not lose their content, confirming the good adhesion of drug/polymer mixtures to the *Carbo*film™ independently of the physicochemical characteristics of the excipient. The TCR percentages recovered from Stent 1 after exposure to human blood at 5, 10 and 15 min were 97.08 ± 1.94, 98.04 ± 1.09 and 96.05 ± 1.30, respectively. In the case of Stent 2 and Stent 6, the differences between the nominal drug content and the experimental percentages recovered after 15 min of exposure to blood were of the same order of magnitude (Stent 2: 96.22 ± 0.41% and Stent 6: 101.61 ± 4.8%).

These results would suggest that the loss of TCR in human blood during the in vivo positioning and deployment procedures is negligible.

3.2. Physical state characterization

TCR is a monohydrated crystal (Fig. 3a) [15], which can be converted in the amorphous form by ultrarapid freezing using lactose as adjuvant [16] or preparing solid dispersion with several polymers such as PVP or HPMC [17]. After the quench cooling of the melted TCR, the glass transition temperature (T_g) was detected at

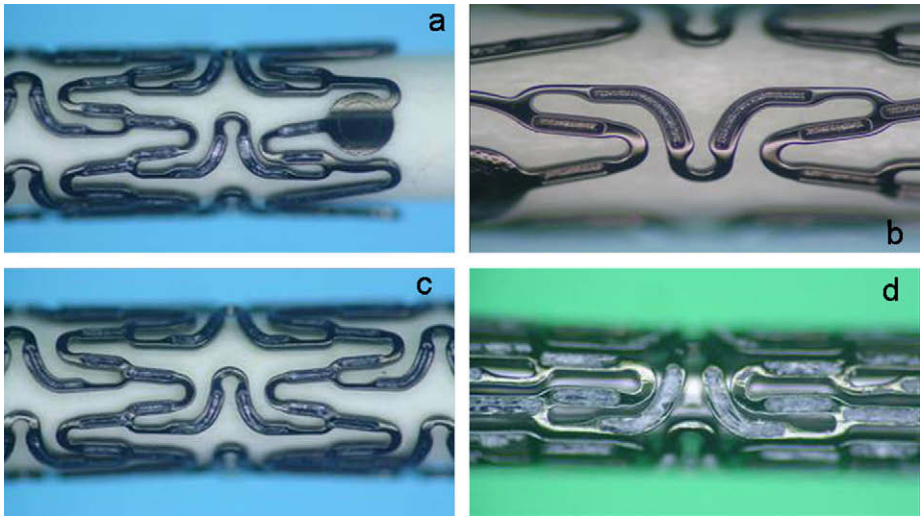

Fig. 2. Optical microscopy images of Stent 1: (a) pre-dissolution, (b) post-dissolution and Stent 2: (c) pre-dissolution and (d) post-dissolution.

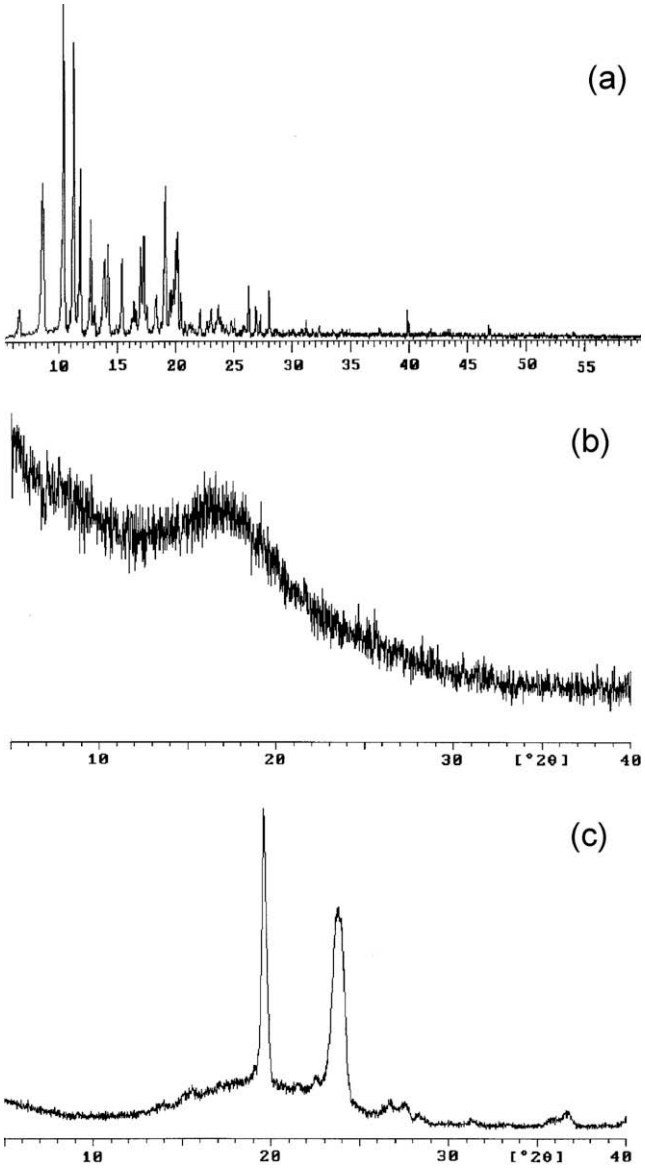

Fig. 3. X-ray diffraction patterns of (a) the monohydrate TCR, (b) TCR after solvent exposure and (c) the TCR/p188 mixture after deposition on *Carbo*film™.

about 77 °C (Fig. 4). The complete amorphization of TCR was also observed after the deposition on the *Carbo*film™ surface. Indeed, the X-ray spectrum did not reveal typical diffraction pattern of the crystalline drug (Fig. 3b). Moreover, after deposition on *Carbo*-film™, TCR remained amorphous more than 1 year of storage in uncontrolled environmental conditions (data not shown).

Fig. 5 shows the ATR–FTIR spectra of TCR as such and TCR deposited on *Carbo*film™ surface. The most diagnostic bands of

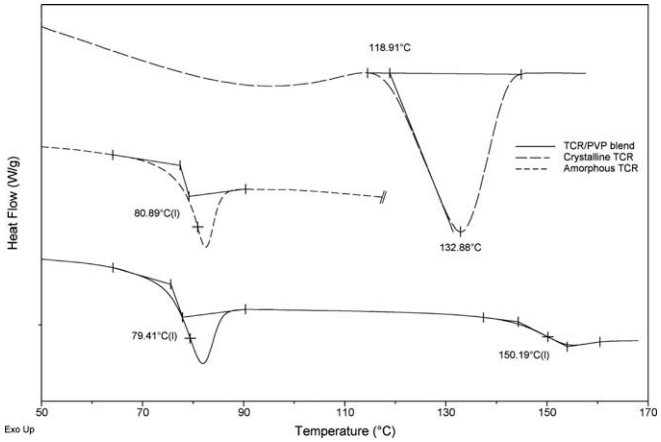

Fig. 4. DSC data of the monohydrate TCR (long dash), amorphous TCR (short dash) and TCR/PVP mixture (solid line).

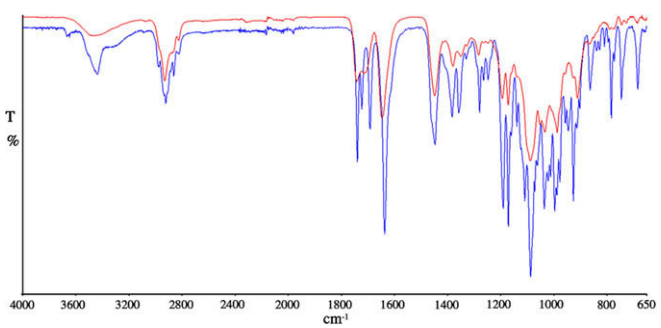

Fig. 5. ATR–FTIR spectra of the monohydrate TCR (blue line) and TCR after deposition on *Carbo*film™ (red line). (For interpretation of the references to colour in this figure legend, the reader is referred to the web version of this article.)

the TCR physical state were the υ-(OH) stretching vibrations in the 3000–3700 cm^{-1} region. In the spectrum of the monohydrate form of TCR, two bands at 3440 cm^{-1} and 3666 cm^{-1} were clearly detectable and attributed to the υ-(OH) of the crystallization water and free hydroxyl groups of TCR, respectively. After deposition on *Carbo*film™ surface, the υ-(OH) stretching band of TCR shifted towards lower wavelength (3470 cm^{-1}) and became broader, indicating the formation of hydrogen bonds. It can be assumed that the formation of hydrogen bonds can be responsible of the stabilization of the amorphous form. This hypothesis is also supported by the shift and the variation in the geometry of the main bands in the υ-(C=O) stretching vibration region.

The surface of the sculptures loaded with TCR (Fig. 6a) or TCR/excipient mixtures had an average roughness ranging from 0.12 to 0.34 nm and appeared homogeneous with the exception of Stent 4, where the roughness estimated from topography images resulted 200 nm and dendrimeric features were evident in the phase data (Fig. 6b). This structure was attributed to the grown of spatial oriented TCR crystals in the p188 matrix. The presence of TCR crystals was also confirmed by the X-ray diffraction pattern of the mixture since two significant bands of the drug were clearly detected (Fig. 3c). No interactions between PVP and the amorphous TCR were assumable since the ATR–FTIR spectra resulted as the sum of the spectra of the two components independently of the drug/excipient ratios. As a matter of fact, DSC data revealed two values of T_g of TCR and PVP at about 77 °C and 140 °C, respectively (Fig. 4). In the ATR–FTIR spectra of the drug/PMM mixtures, the band of the amorphous TCR at 1646 cm^{-1} attributed to the stretching vibration of the amides shifted to 1649 cm^{-1}, and the υ-(C=O) stretching vibration band at 1717 cm^{-1} was not detectable independently of the drug/excipient ratios. Furthermore, the υ-(C=O) bedding bands of PMM at 1145 cm^{-1} and 1240 cm^{-1} shifted towards lower wave numbers (1149 and 1243 cm^{-1}), while the TCR υ-(C=O) bedding bands at 1195 and 1173 cm^{-1} shifted towards higher wave numbers (1192 cm^{-1} and 1171 cm^{-1}). These modifications in the ATR–FTIR spectra suggest that interactions between TCR and PMM had occurred.

3.3. TCR release

3.3.1. In vitro dissolution testing

As expected, the physicochemical features of polymers deeply influenced the released amount over time. The release profiles of TCR from stents loaded by the same ratio of drug/polymer mixtures are shown in Fig. 7. The release rate constant of TCR can be calculated by the general equation:

$$\frac{M_t}{M_\infty} = Kt^n \quad (1)$$

where M_t is the amount of drug released at time t, M_∞ is the amount of drug loaded onto the stent, K is the release rate constant and n is the exponent that determines the order of the equation. Due to the reservoir shape (Fig. 1), it was expected that the TCR release from Stent 1 followed a quasi zero-order kinetic (Eq. (1), $n = 1$) since the exposed surface area would remain constant during the drug release testing. Nevertheless, over the first hours of the experiment, the best fitting model was obtained when n was about 0.5 ($r^2 > 0.99$). The dependence of the drug release profile from the square root of time could be explained considering that a supersaturation of the boundary layer from the amorphous TCR would occur because of its greater solubility with respect to the more stable monohydrate form. However, due to the metastable nature of the amorphous form, a solution-mediated transformation would take place involving an initial nucleation phase followed by the crystal growth to lower the free energy. This hypothesis was confirmed by embedding in water the amorphous TCR deposited onto the *Carbo*film™ over 24 h. The X-ray diffraction data recorded on the dried sample revealed the main diffraction bands of the crystalline phase over the pattern of the amorphous TCR (data not shown). When TCR was mixed with excipients having different physicochemical characteristics, the drug release was governed by two different mechanisms. In the case of PMM, the TCR release was controlled by the diffusion of the drug through an inert matrix. This assumption was also confirmed by visual observation of the DES reservoirs of Stent 2, in which PMM was clearly evident after in vitro release testing (Fig. 2d), with respect to those of Stent 1, which were empty (Fig. 2b). For the mixture containing the water-soluble excipients, namely p188 and PVP, which can be easily hydrated, it was assumed that the TCR release was controlled by the dissolution of the carrier [18]. In both cases, the TCR released fraction from the DESs resulted proportional to the square root of time ($r^2 > 0.98$). The release rate constants (K) calculated according to Eq. (1) ($n = 0.5$) for DES are reported in Table 1. As expected, PMM

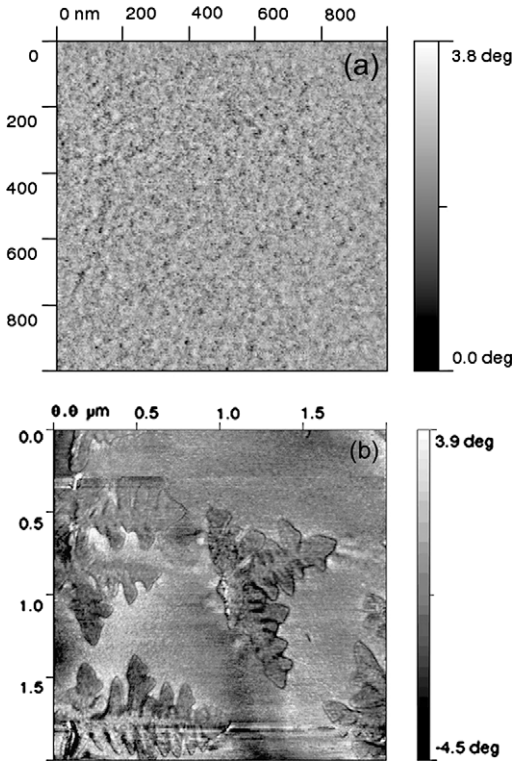

Fig. 6. AFM phase images of (a) TCR (Stent 1) and (b) TCR/p188 mixture (Stent 4) deposited into sculptures of the *Carbo*Stent™.

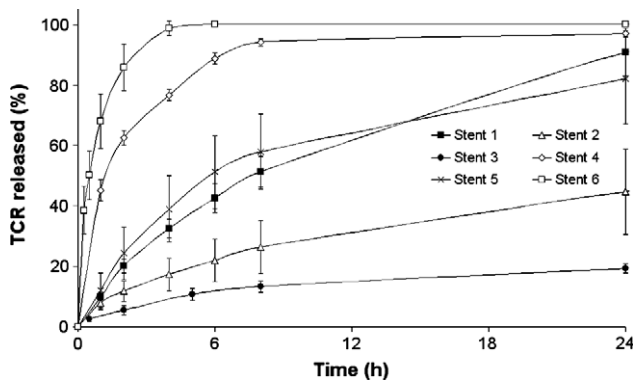

Fig. 7. The release profiles of TCR from stents loaded by TCR/excipient mixtures at the same ratio.

(Stent 2 and Stent 3) significantly decreased the TCR in vitro release rate constants with respect to the stent loaded with only TCR (Stent 1) ($p < 0.008$). The PMM/TCR ratio significantly affected the release rate ($p = 0.039$). As far as the water-soluble excipients are concerned, PVP appeared more effective in enhancing the TCR dissolution rate with respect to p188 at the same TCR/polymer ratio (Fig. 7). This difference may be ascribed to the characteristics of the considered biomaterials as well as the solid state of TCR loaded in the stent's reservoirs. The overall TCR release from Stent 4 appears as the result of two different events: the dissolution of the TCR crystals, which should be slower than the amorphous phase and p188, which should promote and dominate the release of TCR from the stent. Considering that, TCR and PVP were not mixable, the increase in the TCR release rate may be ascribed to the high-intrinsic dissolution rate of the low molecular weight PVP, which enhanced the release of TCR (Table 1). Decreasing PVP/TCR ratio, PVP did not significantly promote the TCR release rate constant with respect to Stent 1, confirming that the TCR release from Stents 5 and 6 is mainly governed by the dissolution of the carrier.

3.3.2. In vivo TCR release

After the deployment of Stents 1–3, no drug was detected in the rabbit blood, confirming the ability to deliver locally, namely in the arterial tissue, a potentially therapeutic concentration of TCR without reaching significant systemic blood levels. The arterial tissue concentrations after Stent 2 and Stent 3 deployment were 42 ± 8 ng/mg and 6 ± 2 ng/mg, respectively, and resulted statistically different ($p = 0.016$). These tissue concentrations resulted lower than those determined by Stent 1 (562 ± 268 ng/mg). The recovery of TCR from DESs after deployment followed the same rank order: the percentages of TCR remained into the reservoirs were 80.0 ± 10.8% and 91.2 ± 7.5% for Stent 1 and Stent 2, respectively. As expected, the amount of TCR recovered from Stent 3 was not different to the theoretical value.

The in vivo TCR tissue concentrations resulted in agreement with the in vitro drug release data. Indeed, the slower the release rates, the lower the TCR concentration in the artery wall.

4. Conclusions

The geometric features of the stent strut and physicochemical characteristics of the *Carbo*film™ resulted suitable to load into the reservoir materials with different physicochemical characteristics. Indeed, mixtures made of TCR and several biomaterials adhered to the *Carbo*film™ and remained into the reservoirs upon exposure to human blood. Generally speaking, the in vitro short-time release test in human blood can be proposed as a useful tool to investigate if during the in vivo interventional procedure a significant loss of a drug would occur. The study provides also information on the TCR physical state and its behavior under different stress conditions. The drug resulted high susceptible to amorphization after quench cooling or evaporation from organic solution. Taking into consideration that the TCR treated by ultrarapid freezing from an acetonitrile/water solution maintained its monohydrated form [16], these results suggest that the stable amorphous phase of TCR can be obtained by treating the drug in absence of water.

References

[1] U. Sigwart, J. Puel, V. Mirkovitch, F. Joffre, L. Kappenberger, Intravascular stents to prevent occlusion and restenosis after transluminal angioplasty, New Engl. J. Med. 316 (1987) 701–706.
[2] B.L. van der Hoeven, N.M.M. Pires, H.M. Warda, P.V. Oemrawsingh, B.J.M. van Vlijmen, P.H.A. Quax, M.J. Schalij, E.E. van der Wall, J.W. Jukema, Drug eluting stents: results promises and problems, Int. J. Cardiol. 99 (2005) 9–17.
[3] N.A. Scott, Restenosis following implantation of bare metal coronary stents: pathophysiology and pathways involved in the vascular response to injury, Adv. Drug Del. Rev. 58 (2006) 358–376.
[4] M.H. Wernick, A. Jeremias, J.P. Carrozza, Drug-eluting stents and stent thrombosis: a cause for concern?, Cor Artery Dis. 17 (2005) 661–665.
[5] H.M. Burt, W.L. Hunter, Drug-eluting stents: a multidisciplinary success story, Adv. Drug Del. Rev. 58 (2006) 350–357.
[6] L. Ge, J. Cosgave, I. Iokovou, G.M. Sangiorgi, A. Colombo, New drug-eluting stent technologies, Curr. Cardiol. Rev. 1 (2005) 953–968.
[7] E.J. Smith, M.T. Rothman, Antiproliferative coatings for the treatment of coronary heart disease: what are the targets and which are the tools, J. Interv. Cardiol. 16 (2003) 475–483.
[8] G. Acharya, K. Park, Mechanisms of controlled drug release from drug eluting stents, Adv. Drug Del. Rev. 58 (2006) 387–401.
[9] A.L. Bartorelli, D. Trabattoni, F. Fabbiocchi, P. Montorsi, S. De Martini, G. Calligaris, G. Teruzzi, S. Galli, P. Ravagnani, Synergy of passive coating and targeted drug delivery: the tacrolimus-eluting Janus CarboStent, J. Interv. Cardiol. 16 (2003) 499–505.
[10] Y.L. Han, S.L. Wang, Q.M. Jing, H.B. Yu, B. Wang, Y.Y. Ma, B. Luan, G. Wang, Midterm outcomes of prospective randomized single-center study of the Janus tacrolimus-eluting stent for treatment of native coronary artery lesions, Chin. Med. J. 120 (2007) 552–556.
[11] J. Garcia-Tejada, H. Gutierrez, A. Albarran, F. Hernandez, T. Velazquez, S. Rodriguez, I. Gomez, J. Tascon, Janus tacrolimus-eluting CarboStent. Immediate and medium-term clinical results, Rev. Espanola Cardiol. 60 (2007) 197–200.
[12] P. Minghetti, Kinetics and the mechanisms of release of target drugs acting against restenosis, in: 14th Annual Transcatheter Cardiovascular Therapeutics Symposium, Washington, DC, September 2002.
[13] N. Kipshide, M.B. Leon, M. Tsapenko, R. Falotico, G. Kopia, J. Moses, Update on Sirolimus drug-eluting stents, Curr. Pharm. Des. 10 (2003) 337–348.
[14] G.W. Stone, S.G. Ellis, D.A. Cox, J. Hermiller, C. O'Shaughnessy, J.T. Mann, M. Turco, R. Caputo, P. Bergin, J. Greenberg, J.J. Popma, M.E. Russell, for the TAXUS-IV Investigators, One-year clinical results with the slow-release polymer-based paclitaxel-eluting TAXUS stent: the TAXUS-IV trial, Circulation 109 (2004) 1942–1947.
[15] H. Taga, H. Tanaka, T. Goto, S. Tada, Structure of a new macrocyclic antibiotic, Acta Crystallogr. C: Cryst. Struct. Commun. C43 (1987) 751–753.
[16] P. Sinswat, K.A. Overhoff, J.T. McConville, K.P. Johnston, R.O. Williams III, Nebulization of nanoparticulate amorphous or crystalline tacrolimus – single dose pharmacokinetics study in mice, Eur. J. Pharm. Biopharm. 69 (2008) 1057–1066.
[17] K. Yamashita, T. Nakate, K. Okimoto, A. Ohike, Y. Tokunaga, R. Ibuki, K. Higaki, T. Kimur, Establishment of new preparation method for solid dispersion formulation of tacrolimus, Int. J. Pharm. 267 (2003) 79–91.
[18] D.Q.M. Craig, The mechanisms of drug release form solid dispersions in water soluble polymers, Int. J. Pharm. 231 (2002) 131–144.